Systems and Control Group

Thesis Systems and Control

Algal growth in horizontal tubular reactors

P.J.M. van Beveren

March 2011

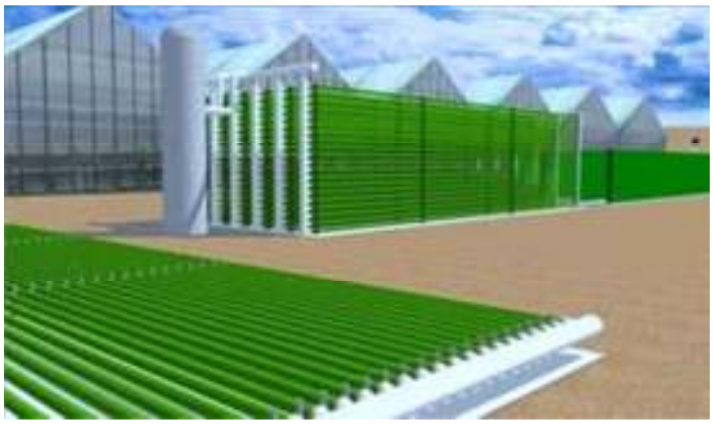

WAGENINGEN UNIVERSITY
AGROTECHNOLOGY AND
FOOD SCIENCES

Algal growth in horizontal tubular reactors

Name course	:	Thesis SCO
Number	:	SCO-80436
Study load	:	36 ECTS
Date	:	March 2011

Student	:	P.J.M. van Beveren
Registration number	:	881026-064-100
Study program	:	MAB (Agricultural and Bioresource Engineering)
Supervisor(s)	:	Ir. P.M. Slegers
		Dr.ir. A.J.B. van Boxtel
Examiner	:	Prof.dr.ir. G. van Straten
Group	:	Systems and Control Group
Address	:	Bornse Weilanden 9
		6708 WG Wageningen
		Tel: (0317) 48 21 24
		Fax: (0317) 48 49 57

WAGENINGEN UNIVERSITY
AGROTECHNOLOGY AND
FOOD SCIENCES

Abstract

Many decision variables are involved in designing and evaluating different algae production systems. For a tubular system i.e. species, latitude, tube diameter, biomass concentration, length of the tubes and the distance between the tubes. To predict yearly biomass production, a model is made to study the effect of these parameters. This model uses reactor characteristics, dynamic sunlight and algae species as inputs. Shading, reflection from the ground and surface, light penetration between tubes and penetration of direct and diffuse light in the algae culture are taken into account. Each tube diameter has a specific optimal biomass concentration for which yearly production is optimal. Maximal tube length is limited by oxygen accumulation. With the presented model maximal tube length as a function of biomass production, and liquid velocity can be determined. For large scale cultivation multiple tubes are placed parallel to each other. From the simulations we conclude that the production per hectare increases with a larger tube diameter and lower biomass concentration (larger volume). With optimisation of the biomass concentration higher production values can be reached.

Table of Contents

1 Introduction

Microalgae are sunlight-driven cell factories that convert carbon dioxide and water into biomass, which contains lipids, proteins and carbohydrates. With this potential microalgae have become an emerging source for the production of biodiesel, biochemicals and food products, which has led to substantial research in this field.

To cultivate algae on a large scale, different types of production systems are used: open systems such as raceway ponds, and closed systems like flat panels and tubular reactors in different configurations. Open and closed systems differ in theoretical maximum yield and production costs. It is generally assumed that despite of a higher yield, the production in closed reactors is much more expensive than in raceway ponds. However, according to Wijffels et al. (2010), the cost price of algae in closed systems will be lower after optimization than in open systems. Realistic estimates for algal production in closed systems are between 40 and 80 tonnes of dry matter per hectare per year (Wijffels et al., 2010). The range for the estimates depends mainly on the technology used, the algae species used, the reactor design and the location of production.

Tubular systems are of interest because they are the most promising systems for scaling up, which is caused by a higher volumetric biomass productivity (Chisti, 2007). Tubular reactors often consist of an array of straight transparent tubes (see Figure 1). The tubes are usually made out of glass or plastic and have a diameter of 0.1 meter or less. Mixing is done via circulation of air and pumping. In Figure 2 a schematic overview of a tubular reactor with a degassing column is shown. Oxygen can leave the system via the degassing column and carbon dioxide is inserted.

Figure 1 Horizontal tubular reactor system without algae. Location: AlgaePARC Wageningen

The maximal areal productivity in tubular reactors ranges from 0.02 to 0.03 $kg.m^{-2}.day^{-1}$ (Del Campo et al., 2001, Rebolloso Fuentes et al., 1999). Due to the tubular shape, there is a high surface-volume ratio which should benefit a higher yield (Posten, 2009). Biomass concentration used in the reactor is strongly related to the tube diameter in such a way that the dark zone must be minimized to limit biomass loss due to respiration (Molina Grima et al., 2001). Areal productivity and volumetric productivity are conflicting parameters for large scale production. A high volumetric production requires a large area to get a high overall production. A high areal productivity means that a the production on an area is very, but the productivity in the volumes used is much lower.

Tube length is limited due to oxygen accumulation in the non-aerated tubes; oxygen accumulation mandates a certain liquid velocity and mixing in a tube of fixed length (Marshall and Huang, 2010). Pumping is usually done by centrifugal pumps or airlift circulators. Medium velocities between 0.20 $m.s^{-1}$ and 0.50 $m.s^{-1}$ are needed to achieve turbulent conditions leading to acceptable light/dark cycles (Posten, 2009).

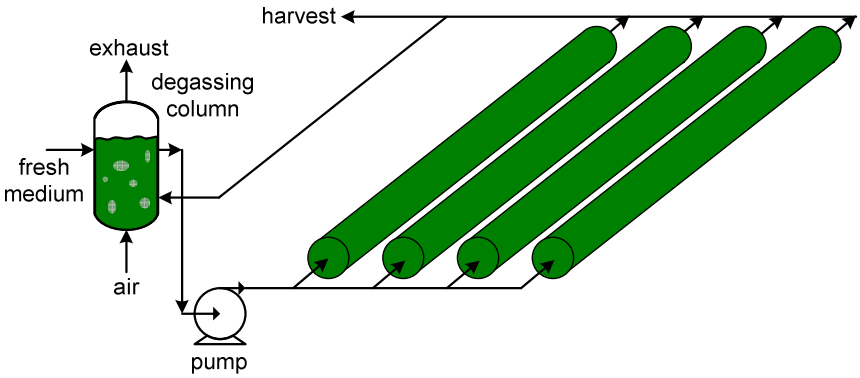

Figure 2. A tubular photobioreactor with parallel horizontal tubes and degassing column (Chisti, 2007). Algae are circulated and led through the degasser where oxygen leaves the system.

The productivity of algae in tubular systems depends thus on design and operational aspects, but also on the available sunlight at the production location which varies over the day and year. At this moment the number of commercially exploited algae cultivation systems and the corresponding productivity data are still limited. Comparing existing systems is not straightforward as the systems are operated under different weather and operational conditions. Therefore, to be able to compare productivity characteristics for differently designed horizontal tubular systems at several locations, a modelling approach is given in this work.

Growth of algae in tubular systems is modelled and simulated for a single tube and for an area of parallel horizontal tubes. The effect of different parameters like location, weather, reactor orientation (north-south and east-west), biomass concentration, length, diameter of the tubes, oxygen accumulation and carbon dioxide uptake in the tubes can be evaluated with the model. Moreover, the model allows optimization towards the best conditions and design for a chosen location.

2 Model description

A mathematical model is needed to evaluate the tubular reactor and get insight in the effect of different parameters. The model calculates the light input on the curved surface of the tube, based on direct, diffuse and reflected light, depending on the place. From this light input the irradiance profile in the tube is calculated. Biomass production is computed from the light profile. In this section, first the structure of the mathematical model (Figure 3) is explained. After that, the decision variables used in the simulations are briefly discussed. An extensive description of the predictive model for single and multiple horizontal parallel tubes can be found in Appendices A and B.

2.1 Mathematical model

Algal growth in a tubular reactor is mainly influenced by the light pattern in the tube. The temperature and the biomass concentration inside the reactor are controlled and assumed to be constant over time, which in practice means that the harvesting rate is equal to the growth rate.

Figure 3 shows the calculation scheme to compute biomass production in a tubular reactor from weather data, reactor design properties, characteristics of algae species and location on earth (latitude) at any time during a day during the year.

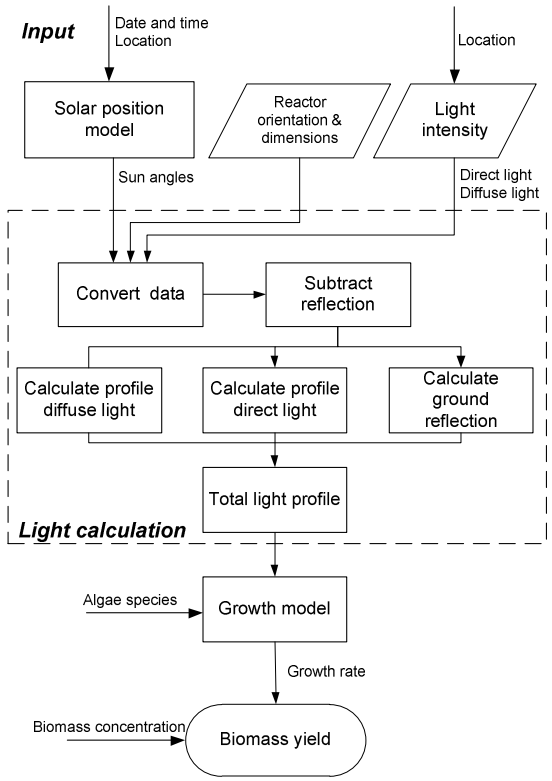

Figure 3. Calculation scheme with parameters and intermediate results to estimate algae production based on solar radiation and design parameters. ▱ = Data, ▭ = Calculation and ⬭ = Result.

To estimate the production on each point in the tube the amount of light on each point should be known. This amount of light depends on the length of the light path and is predicted with the solar position model which calculates the position of the for any time at any position (r_i,φ) on the cross section of the tube. This method is based on the work of Molina Grima et al. (1999) to obtain the local irradiance. An incoming light beam entering a tube is presented in Figure 4. The two main angles that determine solar position are the hour angle on the horizontal plane ω and the elevation angle in the vertical plane α_v. Angle ω in Figure 4 changes with a different reactor orientation γ (see also Appendix A.1.). With these angles known, the length of line P_{direct} is calculated. This line is used later on to calculate the light gradient caused by absorption of light.

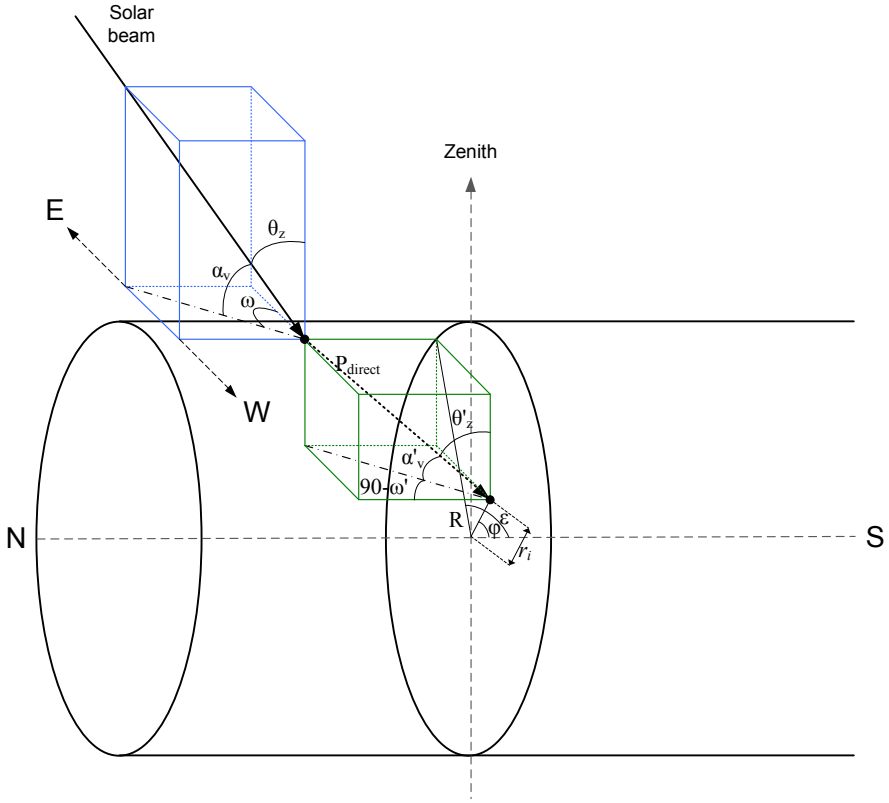

Figure 4. Horizontal tube with direct light beam and corresponding angles associated to the path for any point (r_i,φ) on the cross section of a horizontal tube.

In 'Convert data' the light intensities in the dataset for direct light are measured on a horizontal plane and are corrected to the solar angles. The angles are also corrected to a north-south orientation of the reactor orientation. Another correction is needed to calculate the light profile on the tube surface. This surface is curved, and therefore, the angle of the reactor surface with the earth surface β (see Appendix A.2.) is used to correct the incoming light on a horizontal surface to a tilled surface. The used data contains light intensities for every 10 minutes for different locations, split up in direct and diffuse light.

Reactor characteristics and orientation of the tube (see Appendix A.1.) are taken into account to determine the light profile on the tube surface and the irradiance profile in the cross section of the tube. The total radiation is separated in direct, diffuse and reflected light. Not all light that falls on the reactor reaches the algae culture inside the tube, part of it is reflected by the tube surface. Therefore, the amount of reflected diffuse and direct light by the reactor is subtracted from the incoming light. Another amount of light is reflected by the ground surface and is added to the total incoming light. Lambert-Beer is used to describe the light gradient in the reactor, this is illustrated in Figure 4. The length of the light path is calculated for every point on the cross section for every time step *dt*.

Figure 5 shows the irradiance profile at two times on May 30, 2009 where the movement of the sun over the reactor is clearly visible. Lambert-Beer is applied to calculate the light gradient, so light absorption by the algae is included. The length of the light path used here is derived from the solar angles (see also Figure 4).

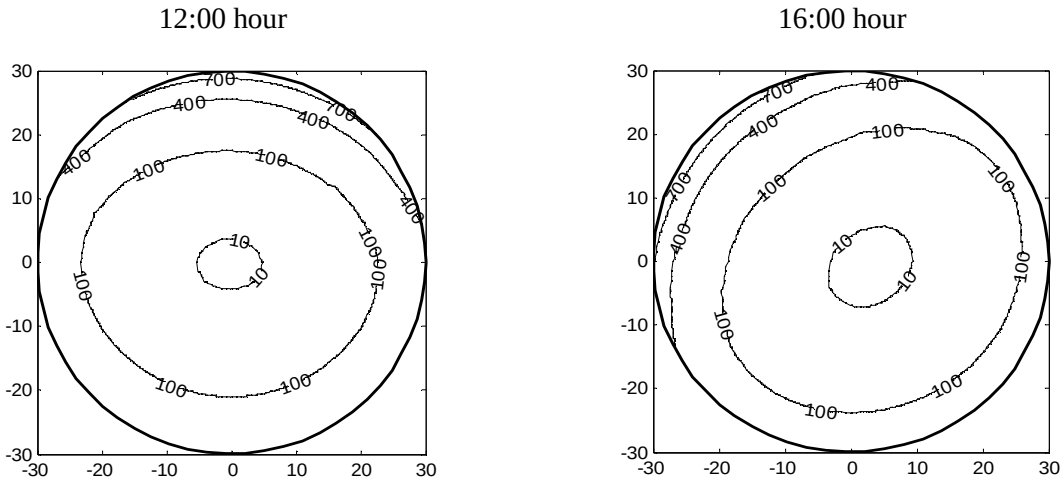

Figure 5. Irradiance profile inside the reactor at 12:00 and 16:00 hour at May 30, 2009 in the Netherlands. Algae species = *P. tricornutum*, reactor orientation = north-south, biomass concentration = 2 kg.m^{-3} and tube diameter = 0.06 m.

The light pattern is used to calculate the growth rate (see Appendix B.). With a known growth rate and biomass concentration the biomass yield is predicted. Algal production is estimated with the growth model of Geider et al. (1996) which is based on *pI*-curves. To acquire realistic estimations of biomass production, radiation data of the World Radiation Monitoring Centre (WMRC) is used as input for the calculations (Knap, 2009, Mimouni, 2009, Morel, 2009).

In case of horizontal parallel tubes there are shading effects and penetration of diffuse light between the tubes. Therefore, direct and diffuse light are corrected for this (see Appendix A.2.). The number and length of the tubes is determined from the total production area (ha) and the distance between the tubes.

Modelling oxygen accumulation and carbon dioxide consumption in a single tube is done with the model for a single tube as described above, except from the assumption that biomass concentration in the tube is constant in the whole reactor. For every part of the tube *dx*, production is calculated and the new biomass concentration is used as input for the calculation of the yield in the next piece of the tube. Stoichiometric factors (see Appendix B) are used to determine the amount of oxygen, carbon dioxide and other components involved in the growth.

2.2 Decision variables

Algal biomass production in tubular reactors is influenced by several decision variables. An overview of the decision variables for production in tubes is given in Table 1. Reactor type and temperature were fixed in this study. Three locations (the Netherlands, France and Algeria) are compared to get insight in the influence of latitude. Others, i.e. tube diameter and biomass concentration were varied to determine their effect on the production. Values are chosen in such a way that effects on the parameter of interest are clearly visible. The remaining operating conditions are assumed to be optimal.

Table 1. Decision variables

Decision variable	Value
Cultivation location	51.97° N, 4.93° E (the Netherlands); 44.08° N, 5.06° E (France); 22.78° N, 5.51° E (Algeria)
Algae species	*Phaeodactylum tricornutum* *Thalassiosira pseudonana*
Reactor type	Tubular PBR
Distance between tubes	0.005-1 m
Tube diameter	0.01-0.07 m
Biomass concentration	0.1 – 10 $kg.m^{-3}$
Temperature	Constant, ideally controlled Optimal: 18° (*T. pseudonana*) [12] 23° (*P. tricornutum*) [12]
Operating conditions	Optimal, ideally mixed

The algae used in the simulations were: *Thalassiosira pseudonana* and *Phaeodactylum tricornutum*, which have a different maximal growth rate and specific light absorption coefficient. Relevant parameter values are listed in Appendix B, Table C.1 and Table C.2.

3 Simulation results

Results of the simulations for biomass production and evaluation of decision variables are presented in the following paragraphs. First, results of the simulations with the single tube are presented, followed by the results of the simulations with multiple tubes. Also the accumulation of oxygen in a single tube is studied.

3.1 Single tubular reactor

A single tube is modelled to investigate the influence of different parameters on the production, without any effect of neighbouring tubes. Fluctuations of algal growth during the year and the effect of decision variables on biomass production are presented.

3.1.1 Yearly biomass production

To examine the algal production on different locations, daily biomass production of *P. tricornutum* is predicted for a tube in the Netherlands, France and Algeria. Daily algal production during one year in the Netherlands is shown in Figure 6, results for France and Algeria are shown in Figure 7 and Figure 8. Standard settings for these simulations are listed in Table 2.

Table 2. Overview of standard decision variables

Decision variable	*P. tricornutum*	*T. pseudonana*
Biomass concentration	1.5 $kg.m^{-3}$	1.0 $kg.m^{-3}$
Reactor orientation	North – south	North – south
Tube diameter	0.06 m	0.06 m
Tube length	100 m	100 m

Production for *P. tricornutum* in the Netherlands reaches a maximum yield in summer of 0.16 kg.tube^{-1}.day^{-1}. Negative productions occur during winter time due to low light levels. Overall production per year is about 20.0 kg.tube^{-1}.year^{-1}. The species *T. pseudonana* shows the same growth pattern, but does not reach as high values for daily biomass production as *P. tricornutum* because of the higher absorption coefficient α. Total production for *T. pseudonana* is about 6.6 kg.tube^{-1}.year^{-1} for given conditions.

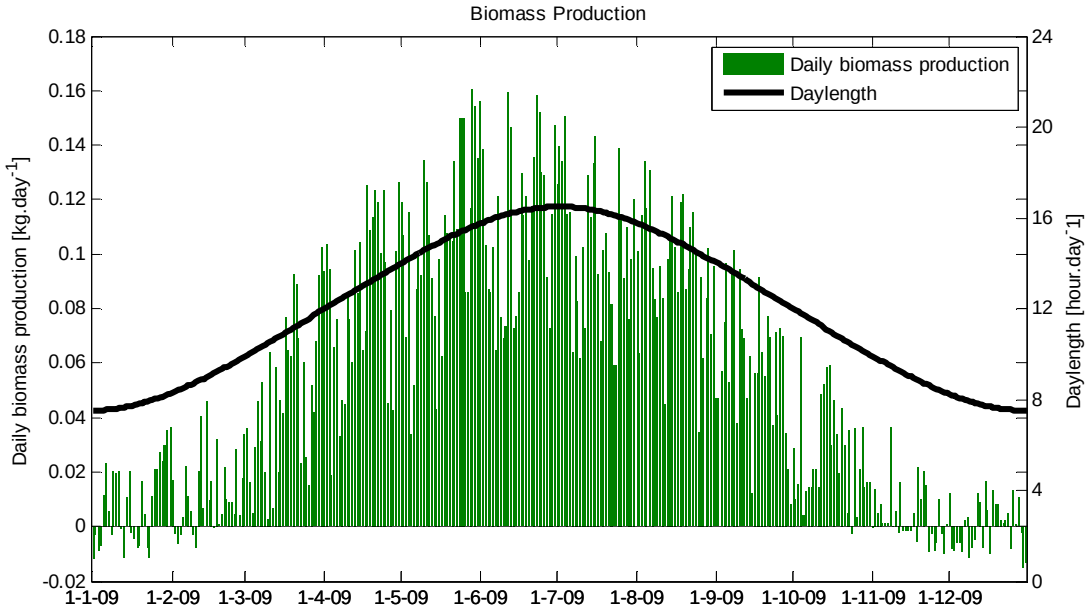

Figure 6. Biomass production in 100 m tube during one year in the Netherlands for *P. tricornutum.*

Production of algae in France shows less days with negative production than in the Netherlands (Figure 7). Due to shorter days in summer, compared to the Netherlands, maximum production is a bit lower in France. Total production for *P. tricornutum* is about 29.2 kg.tube^{-1}.year^{-1} and 11.7 kg.tube^{-1}.year^{-1} for *T. pseudonana*.

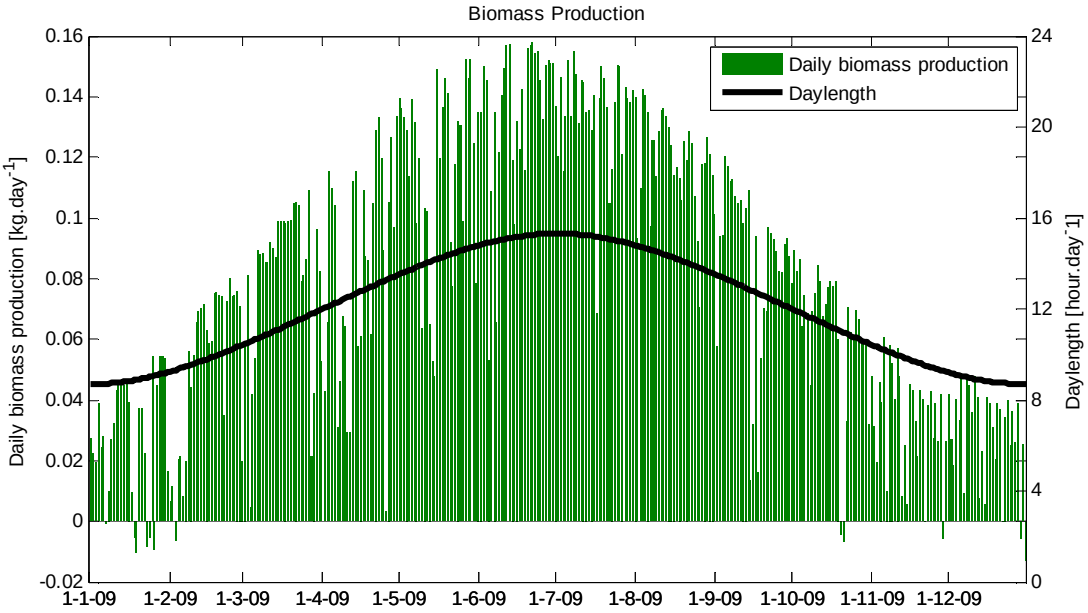

Figure 7. Biomass production in 100 m tube during one year in France for *P. tricornutum.*

Day length in Algeria varies less than in the Netherlands and France, therefore light levels are relatively high in winter (Figure 8). Algal growth is more constant during the year, because algal growth follows the pattern of day length. Total biomass production in Algeria under given conditions will be about 36.8 kg.tube^{-1}.year^{-1} for *P. tricornutum* and 17.0 kg.tube^{-1}.year^{-1} for *T. pseudonana.*

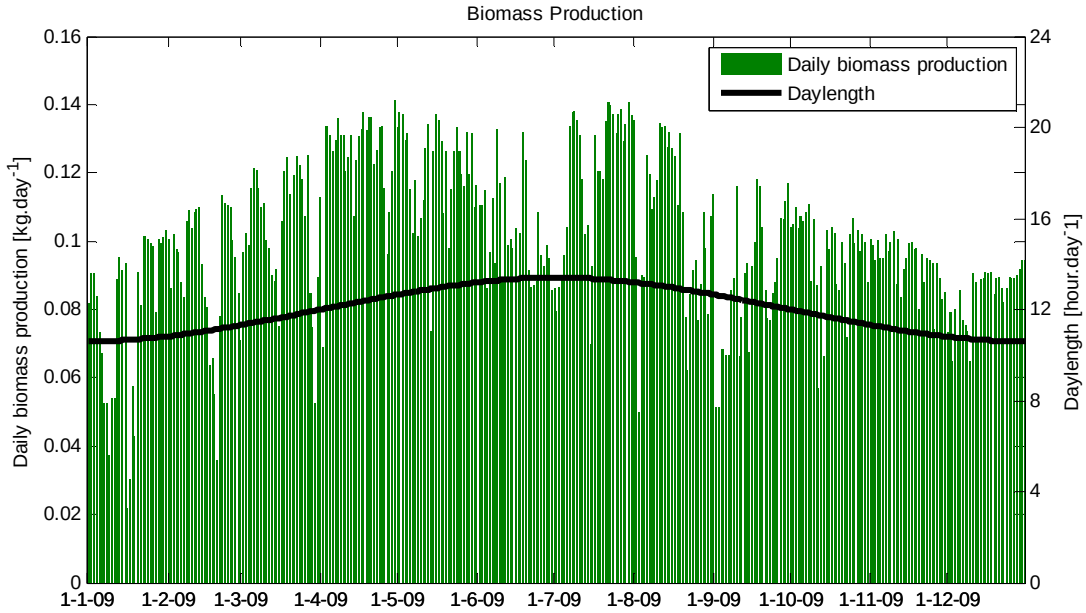

Figure 8. Biomass production in 100 m tube during one year in Algeria for *P. tricornutum.*

Concluding, most production during one year occurs in Algeria. Highest production can be found in the Netherlands during the summer period. Negative production values occur in The Netherlands and France during winter. Algeria shows a more constant production during one year.

3.1.2 Effect of decision variables

A sensitivity analysis is done to get insight in the effect of tube diameter and biomass concentration on the volumetric yearly biomass production. The effect of oxygen accumulation on growth is not yet considered here and growth conditions are assumed to be optimal. All other parameters are as listed in Table 2.

From Figure 9 and Figure 10 follows that in the Netherlands, each tube diameter has a specific yearly constant biomass concentration C_x for which the volumetric production is optimal. As already mentioned before, *P. tricornutum* has an overall higher production compared to *T. pseudonana*. For both species a small tube diameter gives higher production values than a larger diameter, the reason is the higher volume-surface ratio in for the thinner tubes. Production of biomass with *P. tricornutum* is less sensitive to biomass concentration than with *T. pseudonana*; i.e. the C_x of *T. pseudonana* is more critical to obtain a high yearly production. The stronger decrease above the maximal production is caused due to the low light penetration at higher concentrations and the respiration that takes place in the dark areas of the tube.

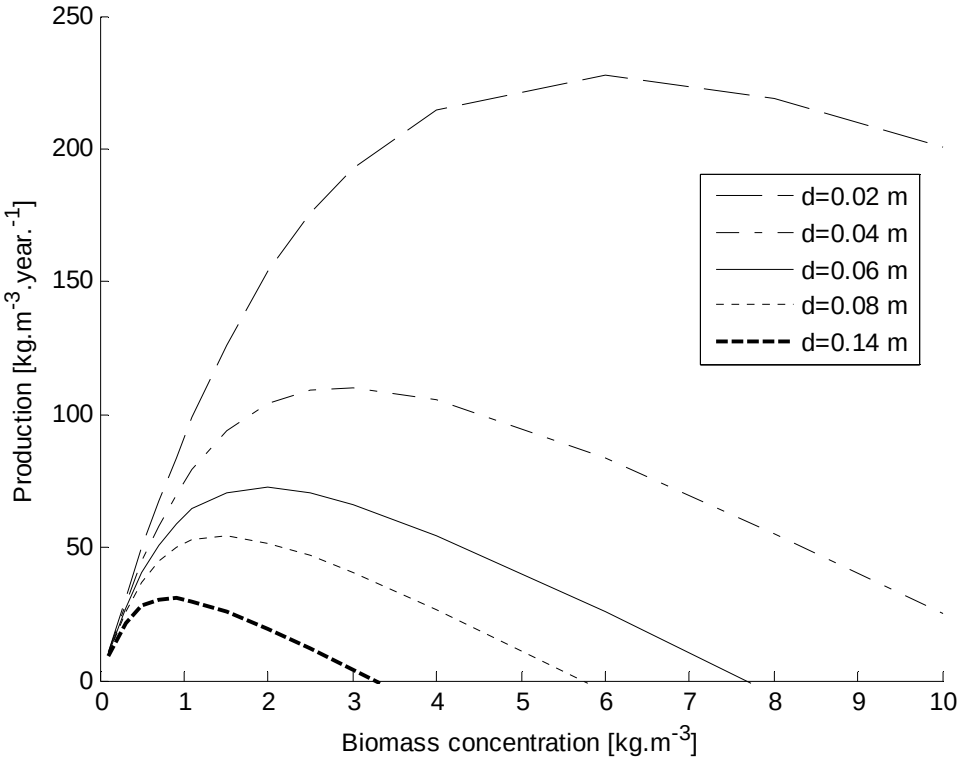

Figure 9. Effect of biomass concentration and tube diameter on yearly volumetric production in the Netherlands. Algae species = *P. tricornutum*.

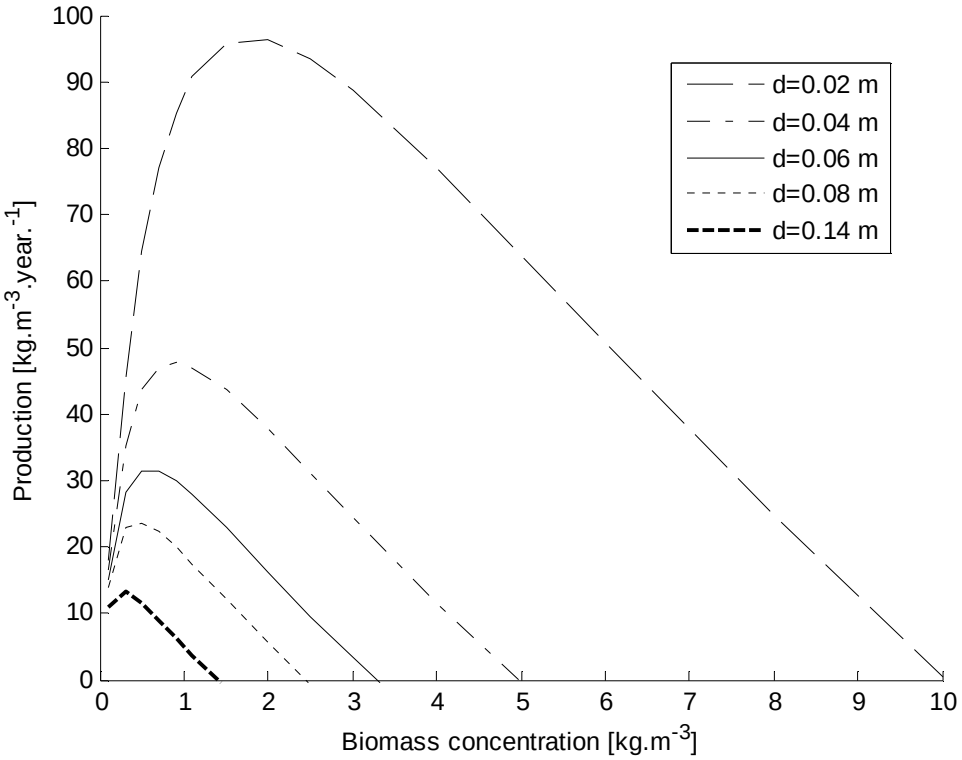

Figure 10. Effect of biomass concentration and tube diameter on yearly volumetric production in the Netherlands. Algae species = *T. pseudonana.*

Similar graphs were obtained for France and Algeria. The curves are, however, shifted. Table 3 gives the yearly biomass productions for which the maximal volumetric production is achieved. These results show that maximal volumetric production increases with a higher biomass concentration and a smaller tube diameter. This holds for both algae species and for the three countries. Algeria shows the overall highest production values for a whole year with a concentration C_x of 8.0 kg.m^{-3} and a tube diameter of 0.02 m.

Table 3. Overview of the combinations for tube diameter and biomass concentration C_x (kg.m^{-3}) that give a maximal yearly volumetric algal production (kg.m^{-3}) for *P. tricornutum* and *T. pseudonana.*

Algae species	*P. tricornutum*					
Country	the Netherlands		France		Algeria	
Tube diameter (m)	C_x	Production	C_x	Production	C_x	Production
0.02	6.0	227.8	6.0	331.8	8.0	436.4
0.04	2.9	110.0	3.0	163.2	4.0	214.6
0.06	2.0	72.6	2.0	108.3	2.5	142.4
0.08	1.5	54.2	1.5	81.0	2.0	106.6
0.14	0.9	30.8	0.9	46.3	1.0	60.0

Algae species	*T. pseudonana*					
Country	the Netherlands		France		Algeria	
Tube diameter (m)	C_x	Production	C_x	Production	C_x	Production
0.02	1.9	96.3	1.9	99.5	2.0	103.6
0.04	0.9	47.7	0.9	48.3	0.9	49.85
0.06	0.7	31.4	0.7	31.7	0.6	32.5
0.08	0.5	23.7	0.5	23.7	0.5	24.1
0.14	0.3	13.5	0.3	13.5	0.3	13.5

In these simulations substrate levels were assumed not to be limiting at every place in the tube. In practice tube length is limited by oxygen accumulation in the tube, and because of that, oxygen accumulation and carbon dioxide uptake in a single tube are simulated.

Simulations were carried out for one single tube to investigate the effect of oxygen on the production in the tube. These simulations are done for a tube with 0.06 m diameter in the Netherlands (see also Figure 10). Two different biomass concentrations (0.5 and 2 kg.m^{-3} at the start of the tube) are used for which yearly biomass production levels vary. The liquid velocity was 0.5 m.s^{-1} and the oxygen concentration at the entrance of the tube equals 100% of air saturation (Molina Grima et al., 2001). This minimal required liquid velocity to acquire turbulent flow is determined by the tube diameter. For a diameter of 0.06 m a liquid velocity of about 0.1 m.s^{-1} is needed to obtain turbulence. The simulation is a worst-case scenario because of the relatively low liquid velocity and the chosen day of simulation; high light levels occur on May 30 at midday. Results of this simulation are shown in Figure 11. The increase in biomass concentration in the tube is very small and therefore, hardly visible in the graph. The tube with a higher biomass concentration and a lower biomass production rate shows a lower accumulation rate of oxygen and therefore, a longer tube could be used. The uptake of carbon dioxide shows the reverse pattern.

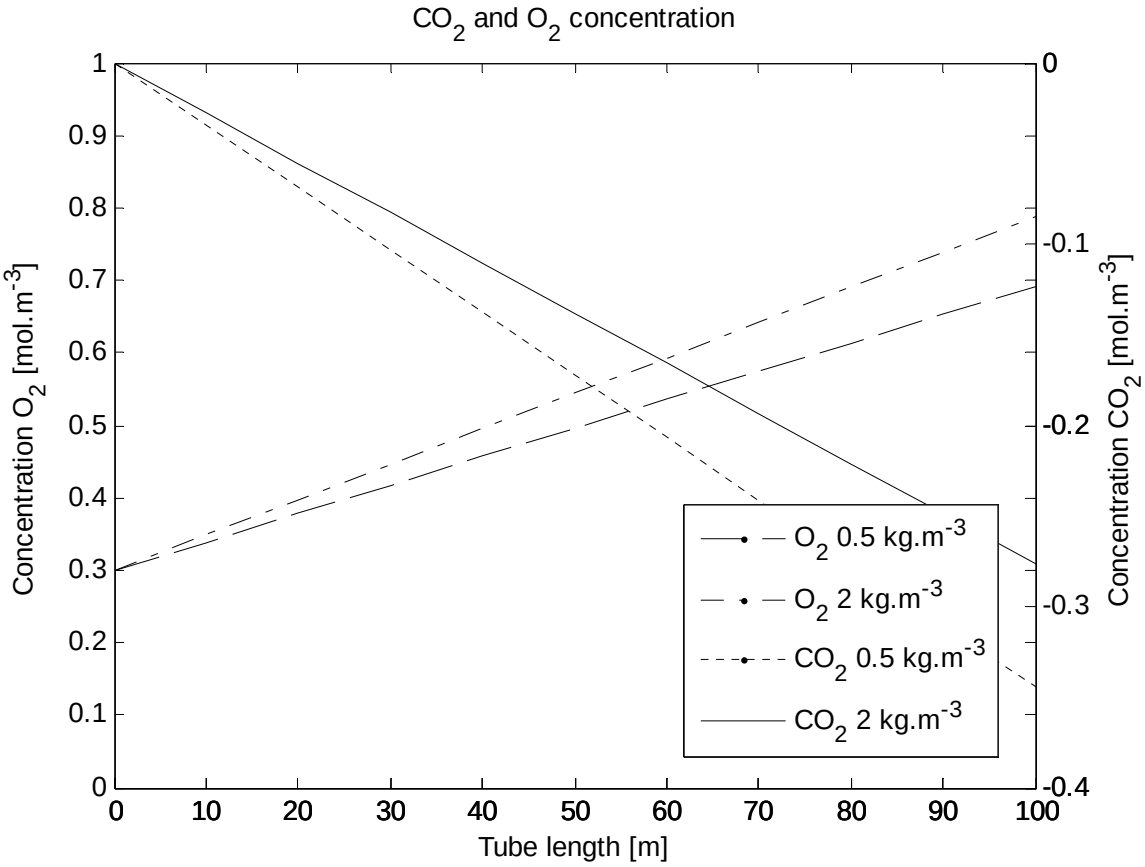

Figure 11. Oxygen and carbon dioxide concentration (mol.m^{-3}) for different biomass concentrations in one single tube at May 30, 2009, 12:00 am in the Netherlands. Tube diameter = 0.06 m, liquid velocity = 0.5 m.s^{-1} and algae species = *P. tricornutum*.

Maximum tube length *L* could also be determined from the equation 1, where tube length "is limited by a combination of the acceptable upper limit on the dissolved oxygen concentration, the liquid velocity through the tube and the rate of photosynthesis" (Acién Fernández et al., 2001). U_L is the liquid velocity (m.s^{-1}) in the tube, $[O_2]_{in}$ and $[O_2]_{out}$ are the dissolved oxygen concentrations (mol.L^{-1}) at the entrance and the outlet of the tube and R_{O_2} is the volumetric rate of oxygen production (mol O_2.m^{-3}.s^{-1}). The formula shows the same results as in the simulation, but only holds for a constant biomass concentration in the tube.

$$L = \frac{U_L([O_2]_{in} - [O_2]_{out})}{R_{O_2}} \quad (1)$$

A level of 300% air saturation of oxygen is assumed to be the maximal value for the oxygen concentration in the tube. With a liquid velocity of 0.5 m.s^{-1} in our simulations this leads to a maximal tube length of 150 m for a biomass concentration of 0.5 kg.m^{-3} and a maximal tube length of 125 m for a concentration of 2 kg.m^{-3}. Oxygen accumulation is less for a biomass concentration of 0.5 kg.m^{-3} because of the lower biomass production. If the concentration C_x in the tube increases, biomass production in the tube will increase and growth also increases with a higher production at a given pipe diameter. The production of oxygen will be lower if the biomass production decreases with an

increasing biomass concentration at given tube diameter. This effect will only be observable with a very low liquid velocity or a very long tube, and is because of that hardly visible in Figure 11.

Besides looking at the oxygen levels on different places at one time moment, it is also interesting to see the behaviour of oxygen production during one day. In Figure 12, the oxygen concentration is simulated at the end of a 100 m tube for different liquid velocities for May 30, 2009 in the Netherlands. Oxygen production is directly related to growth, so it follows the growth pattern. Variations during the day occur due to varying irradiance levels. The oxygen concentration at the end of the tube is higher for lower liquid velocities. The algae have a longer residence time in the tube and therefore, they have more time to grow and more oxygen is accumulated. For countries with higher growth rates during a day, oxygen levels will be higher at the end of the tube. A different tube diameter will also lead to other growth rates and thus also to more or less oxygen build up (according to the results in Figure 10 and Figure 11). Negative oxygen production values occur during night due to respiration. More respiration occurs at a lower liquid velocity and therefore, values at the end of the tube differ during night.

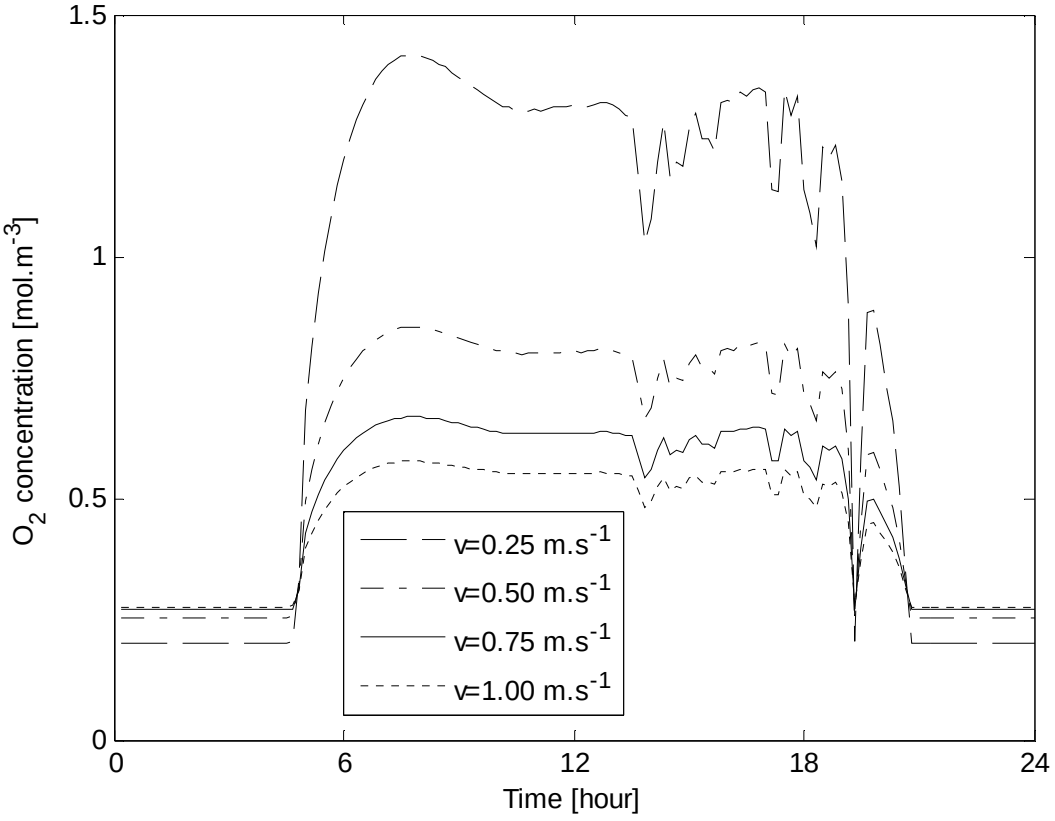

Figure 12. Oxygen concentration (mol.m^{-3}) at the end of a 100 m single tube at different liquid velocities at May 30, 2009 in the Netherlands. Tube diameter = 0.06 m, biomass concentration at the start of the tube = 1.0 kg.m^{-3}, algae species = *P. tricornutum*.

3.2 Multi tubular reactors

For large scale production, multiple tubes can be placed parallel to each other. Placing tubes parallel also implies shading and light penetration effects between tubes (Slegers et al., 2011). These are included in the model for the multi tubular reactors. In this paragraph the yearly algal production for one hectare of tubes is presented for different countries and tube diameters. Also the effect of varying distance between the tubes is studied.

3.2.1 Yearly biomass production

Simulations are done for one hectare of tubes of 100 m, placed with a distance of 0.01 m next to each other. The results for *P. tricornutum* and *T. pseudonana* at different tube diameters are shown in Table 4. The biomass concentrations used are the same as the standard values (Table 2). Algal production with *T. pseudonana* shows less variation than with *P. tricornutum*. The difference in minimum and maximum yearly biomass production in the Netherlands is much bigger for *P. tricornutum*. The optimal tube diameter for *P. tricornutum* at a biomass concentration of 1.5 $kg.m^{-3}$ in the Netherlands is around 0.08 m, while for *T. pseudonana* this diameter is 0.04 m. Other combinations of biomass concentrations and tube distances show the same pattern as in Figure 9 and Figure 10, but with lower production levels.

Table 4. Yearly biomass production (tonnes.year^{-1}) for *P. tricornutum* (C_x = 1.0 kg.m^{-3}) and *T. pseudonana* (C_x = 1.5 kg.m^{-3}) in the Netherlands, France and Algeria for 1 hectare of 100 m tubes. Distance between tubes = 0.01 m, orientation of the tubes = north – south.

	P. tricornutum			*T. pseudonana*		
Diameter (m)	the Netherlands	France	Algeria	the Netherlands	France	Algeria
0.02	12.2	17.5	20.7	9.0	14.2	18.8
0.04	23.5	33.5	41.1	10.9	17.5	24.2
0.06	29.9	42.6	53.8	10.0	17.2	24.9
0.08	32.8	47.1	60.6	8.1	15.7	24.0
0.14	31.5	47.7	64.8	1.4	10.0	19.2

From the diameter of the tubes and the distance between the tubes, the number of tubes of 100 m per hectare can be calculated. A hectare of tubes with a diameter of 0.06 m and the distance between the tubes of 0.01 m contains 1428 tubes. Each tube on this area produces about 96% of the mass production of a single 100 m tube. This holds for the Netherlands, France and Algeria for both algae species.

The biomass concentration used in the previous simulations was kept constant during the year at 1.5 kg.m^{-3}. Optimizing this value gives a concentration of 1.975 kg.m^{-3} and a production of 30.8 tonnes.ha^{-1}.year^{-1} for the Netherlands. Optimizing C_x per month leads to a yield of 32.5 tonnes.ha^{-1}.year^{-1} which is 5.6% more than the optimized production with a fixed optimal concentration. A daily optimization has a potential of about 1.2% extra production on top of the monthly optimized concentration. Optimizing the biomass concentration for different countries will show an increase of the same magnitude.

In addition the biomass concentration per tube diameter is optimized. The results are shown in Figure 13. Yearly areal biomass production increases with a larger tube diameter, while the optimal biomass concentration per year decreases to minimize the dark zone in the tube. Compared to the non-optimized biomass productions (see Table 4) there is no optimum and production still increases till a diameter of 0.16 m.

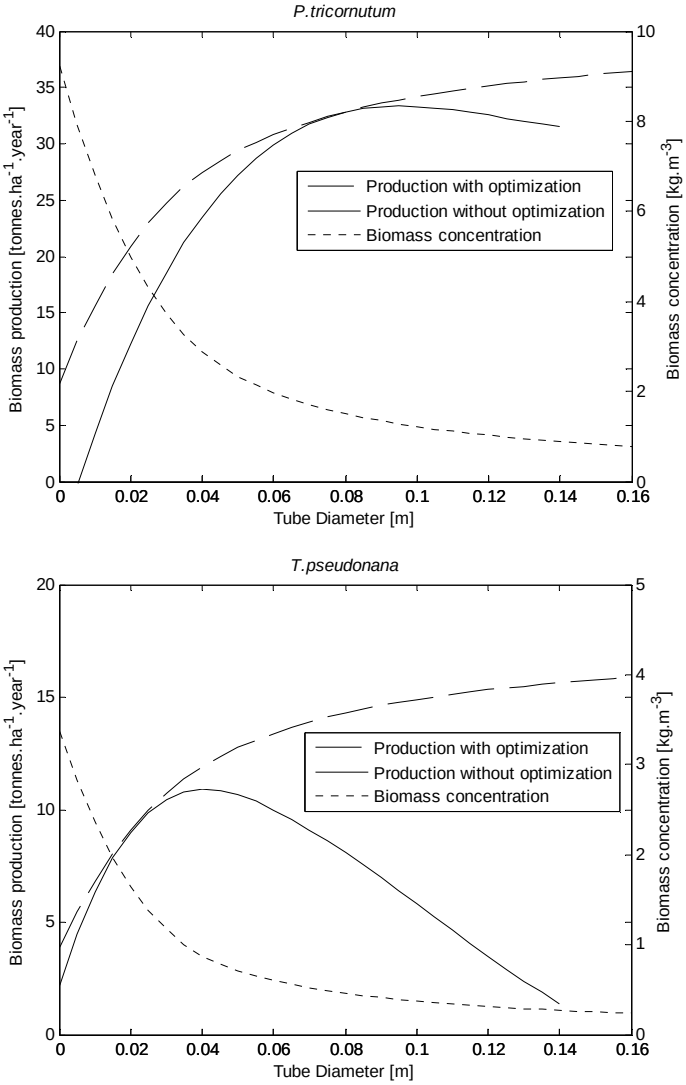

Figure 13 Production at optimized biomass concentrations for *P .tricornutum* (left) and *T. pseudonana* (right) in the Netherlands for different tube diameters.

3.2.2 Influence of distance between tubes

A case of parallel tubes, an extra decision variable is added to the system; the distance between the tubes. In Figure 14 the effect of distance between the tubes on yearly biomass production is shown for both algae species and three different countries. A smaller distance between the tubes leads directly to more biomass production per hectare per year. This means that production benefits more from extra tubes per hectare than from capturing more reflected (by the ground) and diffuse light reaching the bottom of the tube. The same pattern is visible for the three countries as well as for the different algae species.

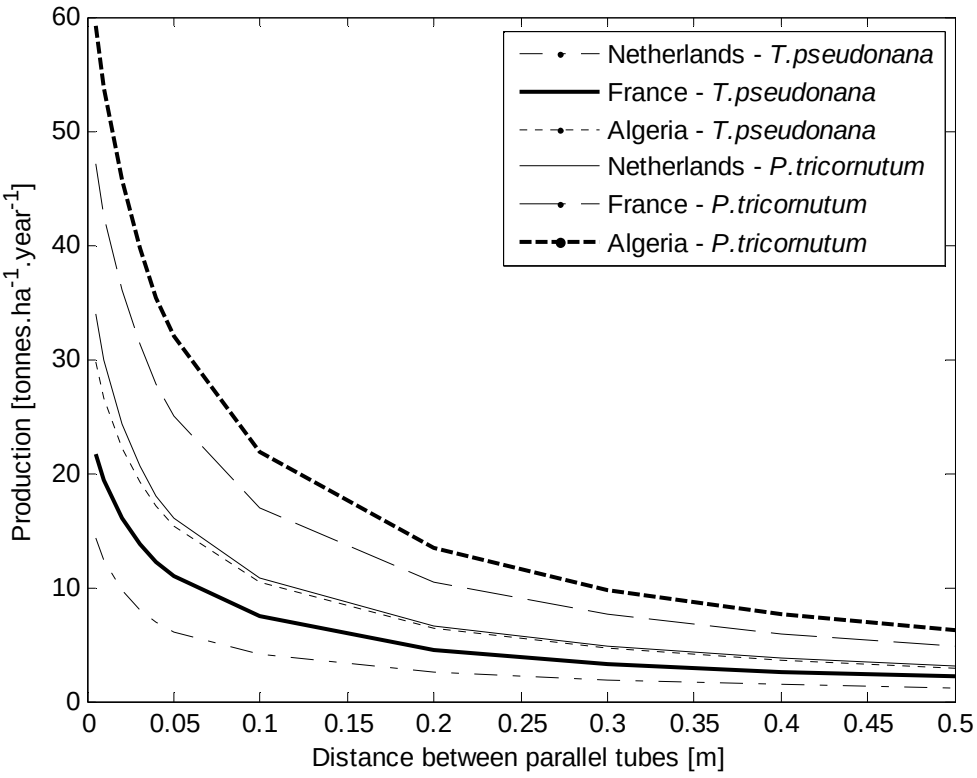

Figure 14. Effect of distance between tubes on yearly biomass production in the Netherlands, France and Algeria for *T. pseudonana* and *P. tricornutum*. Tube diameter = 0.06 m and reactor orientation = north-south.

4 Discussion

Algal biofuel feasibility studies use different numbers for their production estimates. Different productivities are reported in the literature for closed photo bioreactors. Chisti (2007) reports a volumetric productivity of 1.535 $kg.m^{-3}.day^{-1}$, but gives no specifications about the reactor type. Eriksen (2008) gives volumetric productivities between 1.15 and 1.52 $kg.m^{-3}.day^{-1}$, depending on the photosynthetic photo flux density for *P. tricornutum.* Molina Grima et al. (2001) reports values between 1.15 and 1.90 $kg.m^{-3}.day^{-1}$ depending on the day of the year. Ugwu et al. (2008) gives productivities for *P. tricornutum* between 1.20 and 1.90 $kg.m^{-3}.day^{-1}$ for an airlift tubular reactor. These values were obtained at different biomass concentrations or changing biomass concentrations during the year. Highest production values for *P. tricornutum* in our work showed a yearly production of about 227.8 $kg.m^{-3}.year^{-1}$ in the Netherlands and 436.4 $kg.m^{-3}.year^{-1}$ in Algeria. This corresponds to an average productivity of resp. 0.62 and 1.20 $kg.m^{-3}.day^{-1}$. Productivities in summer are of course higher than in winter due to the difference in day length and light intensities. The values from our model give lower estimates than experimental estimates reported before. We must realize us that the values from our model are based on year round simulations. If we look to specific simulated periods, higher and lower productions than average occur. Possibly, the reported values are based on a specific period with beneficial conditions. From this model we learn that using production values from literature could lead to too optimistic production levels. Moreover, the simulated system is a horizontal tubular system, where it is not always clear what kind of reactor is used for the measurements or simulations.

Production has also limiting factors. Research is done on the effect of growth on oxygen levels at different algae species for *Nannochloropsis* (Raso et al., 2011) and *Neochloris oleoabundans* (Sousa et al., 2011). At low light levels, a decrease of about 50% is reported at 200% air saturation for *Nannochloropsis*. At high light levels this decrease already shows up above 100% air saturation. For *Neocloris oleoabundans*, it is found that the effect of oxygen on growth can be overcome by increasing the carbon dioxide level (Sousa et al., 2011) and at high light and oxygen levels, over 500% air saturation, a decrease in growth is observed. These observations show that if more detailed information is available about the effect on growth, this could be included in our prediction models to study the effect on production efficiency.

The effect of liquid velocity on the oxygen and carbon dioxide production was also studied by (Acién Fernández et al., 2001). We found a comparable pattern for the oxygen accumulation during one day for different liquid velocities as they did. Also in the work of (García Camacho et al., 1999) a linear increase of oxygen in the tube is reported. The uptake of carbon dioxide is faster at the begin of the tube, and decreases through the length of the tube. This difference is caused by the change in pH that

is taken into account in the work of (García Camacho et al., 1999). While in our model the pH is assumed to be optimal in the whole tube.

Placing tubes closer to each other in a multiple tube system leads to higher areal productions. More tubes are placed on one hectare, but we observe a decrease in production per tube. The extra yield due to more tubes per hectare delivers more additional production than the extra yield per tube with more light available.

In this research a model is made for horizontally stacked tubes. In practice, also vertically stacked reactors are used. Higher productivities per square meter ground surface could be achieved, but the volumetric productivity could go down than because not all tubes get the same amount of light. Modelling these configuration of tubes gives some more difficulties with calculating light paths, but is a necessary extension to the presented model. Placing the tubes as close as possible to each other could has some analogy with a horizontal plate reactor. Because of the bended surfaces of the tube the surface receiving sunlight is a larger than in case of a plate with the same volume. The work of (Slegers et al., 2011) also shows the relation of light path and biomass concentration on the yearly production. The results for the vertical single flat panel and the horizontal single tube both show optima for the different algae species.

5 Conclusions

Estimating algal biomass production is complex. We have developed a model to predict biomass production in horizontal tubes. Modelling algal growth gives information on the processes and decision variables which play an important role in biomass production. This model provides estimates of algal production in a single tube and on a large scale close to literature data.

Production in a single tube on three different locations is compared to each other: the Netherlands, France and Algeria, and for two algae species: *P. tricornutum* and *T. pseudonana*. Overall, higher production values are reached on locations with a lower latitude and more hours with higher light levels. Each tube diameter has a specific optimal biomass concentration for which the algal production is highest and this varies per latitude. Higher biomass concentrations are beneficial in tubes with a small diameter; this gives a high volumetric productivity. To have a high volumetric productivity relatively more ground area is needed. The main decision variables that determine productivity in the tubular system are the algae species, location and the combination of tube diameter and biomass concentration. Production has also limiting factors. Tube length is limited due to oxygen accumulation. Therefore, the build-up of oxygen in the tube is modelled. The maximum tube length could be estimated based on simulations and given input parameters.

The results for a hectare of horizontal tubes show a same trend for the sensitivity to biomass concentration and tube diameter as single tubes. For a multiple tube system also the distance between the tubes influences the production per hectare. From the model we conclude that areal productivity increases with a smaller distance between the tubes. So, the number of tubes on one hectare will increase. With extra tubes, more algae are produced per year than less tubes with the extra light, due to reflection and diffuse light, could deliver. We have also seen that each tube diameter has a specific optimal biomass concentration for which the production per hectare is highest. Production per hectare increases when for each tube diameter the optimal biomass concentration is chosen, even with large tube diameters and thus lower biomass concentrations. With this research horizontal tubular systems can be evaluated and compared on different aspect and yield predictions for future algae plants can be made.

References

ACIÉN FERNÁNDEZ, F. G., FERNÁNDEZ SEVILLA, J. M., SÁNCHEZ PÉREZ, J. A., MOLINA GRIMA, E. & CHISTI, Y. 2001. Airlift-driven external-loop tubular photobioreactors for outdoor production of microalgae: assessment of design and performance. *Chemical Engineering Science,* 56**,** 2721-2732.

CHISTI, Y. 2007. Biodiesel from microalgae. *Biotechnology Advances,* 25**,** 294-306.

DEL CAMPO, J. A., RODRÍGUEZ, H., MORENO, J., VARGAS, M. Á., RIVAS, J. & GUERRERO, M. G. 2001. Lutein production by Muriellopsis sp. in an outdoor tubular photobioreactor. *Journal of Biotechnology,* 85**,** 289-295.

DUFFIE, J. A. & BECKMAN, W. A. 1991. *Solar engineering of thermal processes,* New York [etc.], Wiley.

ERIKSEN, N. 2008. The technology of microalgal culturing. *Biotechnology Letters,* 30**,** 1525-1536.

GARCÍA CAMACHO, F., CONTRERAS GÓMEZ, A., ACIÉN FERNÁNDEZ, F. G., FERNÁNDEZ SEVILLA, J. & MOLINA GRIMA, E. 1999. Use of concentric-tube airlift photobioreactors for microalgal outdoor mass cultures. *Enzyme and Microbial Technology,* 24**,** 164-172.

GEIDER, R. J., MACINTYRE, H. L. & KANA, T. M. 1996. A Dynamic Model of Photoadaptation in Phytoplankton. *Limnology and Oceanography,* 41**,** 1-15.

KNAP, W. 2009. Basic measurements of radiation at station Cabauw , Koninklijk Nederlands Meteorologisch Instituut, De Bilt.

LIU, B. Y. H. & JORDAN, R. C. 1960. The interrelationship and characteristic distribution of direct, diffuse and total solar radiation. *Solar Energy,* 4**,** 1-19.

MARSHALL, J. S. & HUANG, Y. 2010. Simulation of light-limited algae growth in homogeneous turbulence. *Chemical Engineering Science,* 65**,** 3865-3875.

MIMOUNI, M. 2009. Basic measurements of radiation at station Tamanrasset , National Meteorological Office of Algeria.

MOLINA GRIMA, E., FERNÁNDEZ, F. G. A., GARCÍA CAMACHO, F. & CHISTI, Y. 1999. Photobioreactors: light regime, mass transfer, and scaleup. *Journal of Biotechnology,* 70**,** 231-247.

MOLINA GRIMA, E., FERNÁNDEZ, J., ACIÉN, F. G. & CHISTI, Y. 2001. Tubular photobioreactor design for algal cultures. *Journal of Biotechnology,* 92**,** 113-131.

MOREL, J.-P. 2009. Basic measurements of radiation at station Carpentras , Centre Radiometrique.

POSTEN, C. 2009. Design principles of photo-bioreactors for cultivation of microalgae. *Engineering in Life Sciences,* 9**,** 165-177.

RASO, S., VAN GENUGTEN, B., VERMUË, M. & WIJFFELS, R. H. 2011. Effect of oxygen concentration on the growth of Nannochloropsis sp. at low light intensity. Wageningen: Wageningen University.

REBOLLOSO FUENTES, M. M., GARCIA SÁNCHEZ, J. L., FERNÁNDEZ SEVILLA, J. M., ACIÉN FERNÁNDEZ, F. G., SÁNCHEZ PÉREZ, J. A., MOLINA GRIMA, E., R. OSINGA, J. T. J. G. B. & WIJFFELS, R. H. 1999. Outdoor continuous culture of Porphyridium cruentum in a tubular photobioreactor: quantitative analysis of the daily cyclic variation of culture parameters. *Progress in Industrial Microbiology.* Elsevier.

SLEGERS, P. M., WIJFFELS, R. H., VAN STRATEN, G. & VAN BOXTEL, A. J. B. 2011. Design scenarios for flat panel photobioreactors. *Applied Energy,* In Press, Corrected Proof.

SOUSA, C., DE WINTER, L., JANSSEN, M., VERMUE, M. & WIJFFELS, R. H. 2011. Effect of oxygen partial pressure and oxygen carbon dioxide ratio on microalgal growth at sub-saturating light intensities. Wageningen: Wageningen University.

UGWU, C. U., AOYAGI, H. & UCHIYAMA, H. 2008. Photobioreactors for mass cultivation of algae. *Bioresource Technology,* 99**,** 4021-4028.

WIJFFELS, R. H., BARBOSA, M. J. & EPPINK, M. H. M. 2010. Microalgae for the production of bulk chemicals and biofuels. *Biofuels, Bioproducts and Biorefining,* 4**,** 287-295.

Appendix

A. Light

A.1. Solar incidence angle

Direct light falling on a tubular reactor varies with the solar position. To determine the solar incidence angle, the same model for solar position is used as in (Slegers et al., 2011) . The solar incidence angle θ on a tubular reactor depends on the solar declination δ which is angular position of the sun at solar noon with respect to the plane of the equator, the latitude of the reactor location θ, the slope of the reactor with respect to the ground surface β, the surface azimuth angle between the normal of the reactor surface and south γ and the solar hour angle ω. Figure A.1.1. gives an overview of the parameters involved in the calculation of the solar incidence angle θ:

$$\cos(\theta) = \sin(\delta)\cdot\sin(\varphi)\cdot\cos(\beta) - \sin(\delta)\cdot\cos(\varphi)\cdot\sin(\beta)\cdot\cos(\gamma) + \cos(\delta)\cdot\cos(\varphi)\cdot\cos(\beta)\cdot\cos(\omega) + \cos(\delta)\cdot\sin(\varphi)\cdot\sin(\beta)\cdot\cos(\gamma)\cdot\cos(\omega) + \cos(\delta)\cdot\sin(\beta)\cdot\sin(\gamma)\cdot\sin(\omega) \quad \text{(A.1)}$$

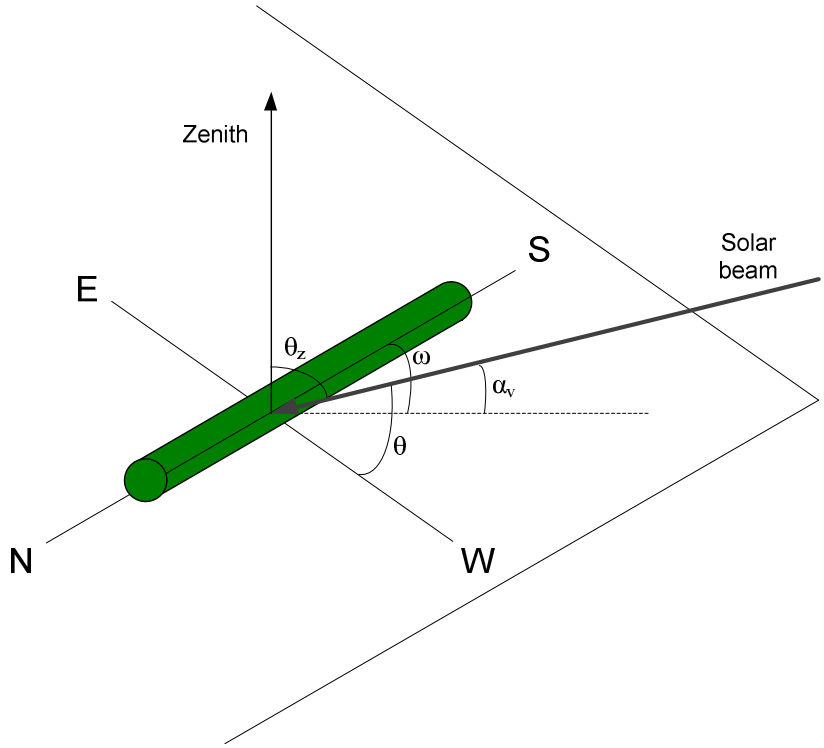

Figure A.1.1. Light beam falling on tubular reactor with different angles.

The angles β, γ are fixed during time (these are reactor characteristics), the angle ω depends on the solar hour and angle δ on the day of the year.

The solar declination δ for equation A.1 varies with the day number in the year *N:*

$$\delta = 23.45\cdot\sin\left(\frac{360(284+N}{365}\right) \quad \text{(A.2)}$$

and the solar hour angle, which is displacement of the sun from the local meridian ω in

equation A.3, is given by

$$\omega = 15(t_{solar} - 12) \tag{A.3}$$

in which the solar time t_{solar} (h) depends on the actual time t, longitude of the reactor location λ, the meridian of the reactor location κ and the equation of time e (see Equation A.4-A.6):

$$\zeta = (N - 1)\frac{360}{365} \tag{A.4}$$

$$e = 229.2 \cdot (0.000075 + 0.001868 \cdot \cos(\zeta) - 0.032077 \cdot \sin(\zeta) - 0.014615 \cdot \cos(2 \cdot \zeta) - 0.04089 \cdot \sin(2 \cdot \zeta) \tag{A.5}$$

$$t_{solar} = t + \frac{4 \cdot (\lambda - \kappa) + e}{60} \tag{A.6}$$

The zenith angle θ_z (°) and the solar elevation angle α_v (°) in Figure A.1.1 are given by :

$$\cos(\theta_z) = \sin(\varphi) \cdot \sin(\delta) + \cos(\varphi) \cdot \cos(\delta) \cdot \cos(\omega) \tag{A.7}$$

$$\alpha_v = 90 - \theta_z \tag{A.8}$$

The orientation γ of the reactor is shown in Figure A.1.2. for two situations. The orientation is the angle measured from the normal of the reactor to the south on the horizontal plane and is positive for a position in the S-E and N-W direction and negative for a position in S-W and N-E. Angle ω is the hour angle and is negative in the morning and positive in the afternoon.

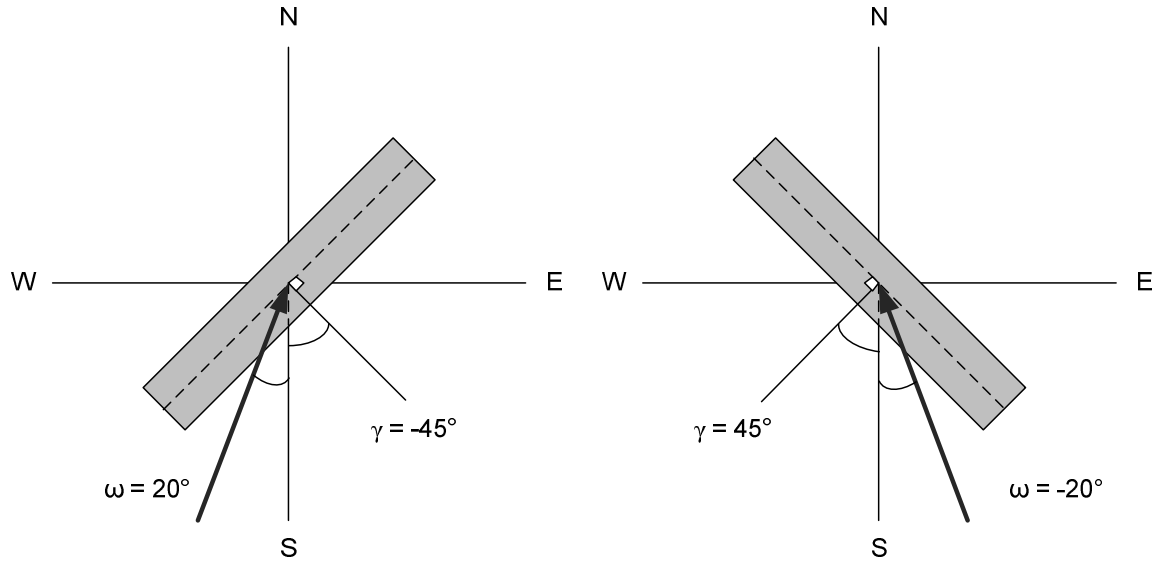

Figure A.1.2. Reactor orientation γ and hour angle ω for two situations γ = -45° (left) and γ = -45° (right).

A.2. Light input single tube

The data for direct light is measured perpendicular to the incoming light beam. Therefore a correction is needed to calculate the light level on the horizontal plane. This is done by multiplying incoming direct light with the cosine of the solar zenith angle (Equation A.9). I_{direct} is the measured direct light available from the dataset and $I_{hor.direct}$ is the corrected amount of direct light. Each point at the tube's contour has a different angle of the reactor surface β, so correction is needed to calculate the light profile on the surface. Correction for the tilted surface angle β (see Figure A.2.1.) is done with equation A.10 (Liu and Jordan, 1960) where G_{direct} and $G_{diffuse}$ are geometric factors. Total radiation on the tubes surface is calculated by Equation A.19.

$$I_{hor.direct}(\beta, t) = I_{direct} \cdot \cos(\theta_z) \tag{A.9}$$

$$\mathrm{G}_{direct}(\beta) = \frac{\cos(\theta(\beta, \gamma))}{\cos(\theta_z)} \tag{A.10}$$

A correction for diffuse sky light is also needed. This factor is a function of the reactor surface angle β and the sky view angle u to correct for diffuse sky light penetration:

$$\mathrm{G}_{diffuse} = \frac{1 + \cos(\beta + u)}{2} \tag{A.11}$$

In which u is a function of the height of the reactor h and the distance between the tubes τ (see Figure A.2.1)*:*

$$\mathrm{u} = tan^{-1}\left(\frac{h}{\tau}\right) \tag{A.12}$$

for multiple tubes and u = 0 for a single tube.

The tubes at the border of the algae plant have a different light pattern. For a large scale production we assume that this effect is negligible and all tubes are treated similarly in the simulations. Ground reflection only occurs if the sun is above a certain height that direct light can hit the ground, depending on the angles of the sun.

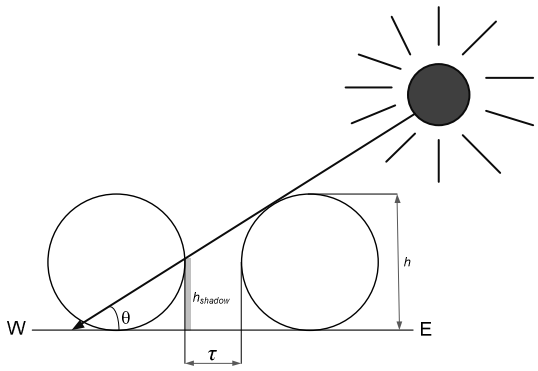

Figure A.2.1. Illustration of the shadow area in the tube and reflection via the ground.

Angle β is illustrated in Figure A.2.1. where ε is the angle, combined with the radius R, describing each point on the surface expressed in polar coordinates. Ground reflected light also contributes to the total amount of light falling on the reactor. Therefore, the amount of light reflected by the ground is added to the total amount of light (Equation A.19).

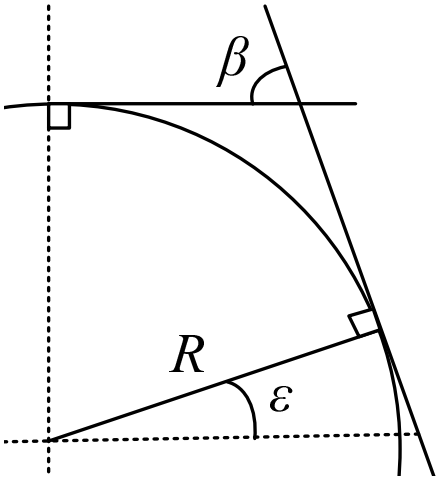

Figure A.2.2. Illustration of angle β to calculate the diffuse light profile on the tube surface.

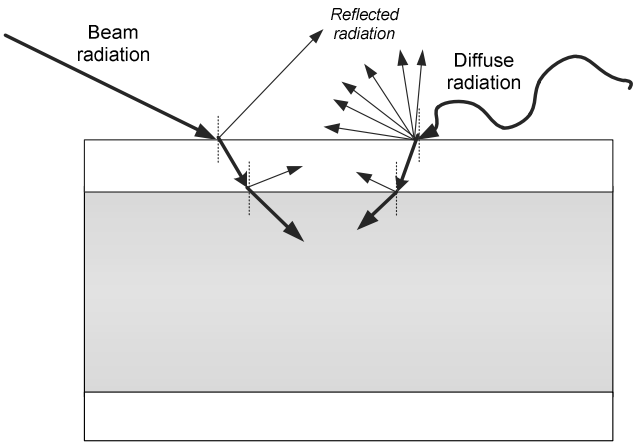

Figure A.2.3. Longitudinal section of a tube with incoming light falling on the tube and light losses due to reflection.

Not all the light that falls on the reactor surface reaches the algae inside the tube. Losses occur due to reflection of different material interfaces: light from the air to the reactor material (glass) and from glass to the algae solution. The amount of reflected light depends on the difference in refractive index of the two interfaces. Diffuse light penetrates the reactor from any direction that is why the reflected radiation could have any direction as well. Reflection of direct light occurs in one certain direction (Figure A.2.3.). The angle of refracted light to the normal is calculated with Snell's law (Equation A.13). For diffuse light, an angle of 60° is assumed to be angle of incidence (Duffie and Beckman, 1991).

$$\frac{\mathrm{Sin}(\theta_i)}{\sin(\theta_t)} = \frac{n_t}{n_i} \qquad \text{(A.13)}$$

The amount of reflection by the tube follows from the Fresnel equations (Equation A.14 and A.15). The reflection of s-polarized light R_s is given by Equation (A.14) and reflection of p-polarized light R_p by Equation (A.15). n_i and n_t are the refractive indices of the material before and after the interface, θ_i is the angle of incidence and θ_t is the angle of refraction measured to the normal of the surface.

$$R_s = \left(\frac{n_i \cdot \cos(\theta_i) - n_t \cdot \sqrt{1 - \left(\frac{n_i}{n_t} \cdot \sin(\theta_i)^2\right)}}{n_i \cdot \cos(\theta_i) + n_t \cdot \sqrt{1 - \left(\frac{n_i}{n_t} \cdot \sin(\theta_i)^2\right)}} \right)^2 \quad \text{(A.14)}$$

$$R_p = \left(\frac{n_i \cdot \sqrt{1 - \left(\frac{n_i}{n_t} \cdot \sin(\theta_i)^2\right)} - n_t \cdot \cos(\theta_i)}{n_i \cdot \sqrt{1 - \left(\frac{n_i}{n_t} \cdot \sin(\theta_i)^2\right)} + n_t \cdot \cos(\theta_i)} \right)^2 \quad \text{(A.15)}$$

Because normal sunlight is not polarized, it is necessary to adapt the results of the Fresnel equations to the right conditions. Therefore, the average of the reflection coefficients R_{tot} for s- and p-polarized light is used (Equation A.16).

$$R_{tot} = \frac{R_s + R_p}{2} \quad \text{(A.16)}$$

The amount of reflected light calculated with the Fresnel equations, does not contribute to growth in the tube, so this amount of light must be subtracted from the total amount of light. This is done by Equations A.17 and A.18 where the amount of light is multiplied by one minus the fraction reflected R for direct and diffuse light separately. $I_{direct.reflected.tube}$ and $I_{diffuse.reflected.tube}$ are respectively the amount of light reflected by the surface of the tube for direct and diffuse light fraction of the light.

$$I_{direct,reflected,tube} = I_{hor.direct} \cdot G_{direct} \cdot (1 - R_{tot.direct}) \quad \text{(A.17)}$$

$$I_{diffuse,reflected,tube} = I_{diffuse} \cdot G_{diffuse} \cdot \left(1 - R_{tot.diffuse}\right) \quad \text{(A.18)}$$

From all corrections and calculations before the total amount of light on the reactor surface is calculated for direct light $I_{total.direct}$ and diffuse light $I_{total.diffuse}$:

$$I_{total,direct}(\beta, t) = \mathrm{G}_{direct}(\beta) \cdot I_{hor.direct}(\mathrm{t}) - I_{direct,reflected,tube}(t) \quad \text{(A.19)}$$

$$I_{total,diffuse}(\beta, t) = \mathrm{G}_{diffuse}(\beta) \cdot I_{hor.diffuse}(t) + I_{refelected,ground}(t) - I_{diffuse,reflected,tube}(t) \quad \text{(A.20)}$$

From the total light input on the tubes surface the length of the light path is calculated. P_{direct} is based on non-refracted light. From this length P_{direct}, the biomass concentration C_x, the absorption coefficient K_a the local irradiance is calculated with Equation A.23 and A.24.

$$I_{local.direct}(r_i, \varepsilon) = I_{total.direct} \cdot \mathrm{e}^{-K_a \cdot C_x \cdot P_{direct}} \quad \text{(A.21)}$$

$$I_{local.diffuse}(r_i, \varepsilon) = I_{total.diffuse} \cdot \mathrm{e}^{-K_a \cdot C_x \cdot P_{direct}} \quad \text{(A.22)}$$

The total irradiance $I_{total.irradiance}$ at each point in the tube is than calculated with Equation A.25

$$I_{total.irradiance}(r_i, \varepsilon) = I_{local.direct} + I_{local.diffuse} \quad \text{(A.23)}$$

B. Algae

B.1. Algal productivity

The accumulation of algae biomass in the reactor as function of the time is given in Equation B.1. The biomass concentration C_x is assumed to be constant in the reactor. The overall growth rate μ therefore equals the dilution rate *D*. This assumption leads to a small overestimation. Growth is calculated for every point in the circle.

$$\frac{\mathrm{D}C_x(t)}{dt} = (\mu(t) - D(t)) \cdot C_x(t) \tag{B.1}$$

The growth model used in this simulations is the model of (Geider et al., 1996). This model is valid for an ideally mixed system at constant optimal temperature.

$$\mu(y,z,t) = {P^C}_m \left(1 - e^{\left(\frac{-\sigma \cdot \mathrm{I} \cdot (y,z,t) \cdot \Theta(y,z,t)}{{P^C}_m}\right)}\right) - r_m \tag{B.2}$$

With: ${P^C}_m = \mu_{\max} + r_m$

The overall/net growth rate μ depends on the maximal chlorophyll *a* and carbon ratio in the cell Θ_{max}, the functional cross section of the photosynthetic apparatus σ, local irradiance $I_{local.irrandiance}$ and the maximum carbon specific rate of photosynthesis P_m^C.

The chlorophyll *a*:carbon ratio is given by:

$$\Theta(y,z,t,) = \Theta_{max} \cdot \frac{1}{1 + \frac{\Theta_{max} \cdot \sigma \cdot I_{local.irradiance}(y,z,t)}{2 \cdot P_m^C}} \tag{B.3}$$

With Θ_{max} the maximal chlorophyll *a*:carbon ratio

All the used parameters are listed in Table C.1 and Table C.2.

B.2. Substrate consumption and oxygen production

Stoichiometric factors are used to determine the substrate consumption rates and the oxygen production rate from the biomass production rate. The reaction stoichiometry is based on the values in Table.

The reaction stoichiometry for growth of *P. tricornutum* on nitric and phosphoric acid is:

$CO_2 + 0.1181\ HNO_3 + 0.7800\ H_2O + 0.068\ H_3PO_4 \rightarrow CH_{1.6985}O_{0.3291}N_{0.1181}P_{0.0068} + 1.41622\ O_2$

and for growth of *T. pseudonana*:

$CO_2 + 0.1564\ HNO_3 + 0.7381\ H_2O + 0.0125\ H_3PO_4 \rightarrow CH_{1.6701}O_{0.3150}N_{0.1564}P_{0.0125} + 1.4712\ O_2$

To calculate the accumulation of oxygen on each place in the tube Equation B.2.1 is used where $\frac{dC_x}{dx}$ is the increase in biomass concentration per unit of length and *v* the liquid velocity.

$$\frac{dC_x}{dt} = \mu(t) \cdot C_x(x,t) + v \cdot \frac{dC_x(t)}{dx} \quad \text{(B.4)}$$

Table B.1 Overview of general parameters.

Parameter	Value
η_{air}	1.0008
$\eta_{algaesolution}$(water)	1.51
$\eta_{reactorwall}$(glass)	1.33
$\theta_{i,diffuse}$	60°

Table B.2 Algae specific parameters.

Parameter	*T. pseudonana*	*P. tricornutum*	Dimensions
K_a	269	75	$m^2.kg^{-1}$
μ_{max}	3.29	1.4	day^{-1}
R_m	0.05	0.05	day^{-1}
σ	10	10	$m^2.mol^{-1}$ photons
Θ_{max}	0.08	0.08	g Chl a g^{-1} C
T_{opt}	18	23	°C
Biochemical composition	14-20-33	11-20-56	Carbohydrates-lipids-proteins
Average phosphor – carbon ratio	1:80	1:147	-

C. Nomenclature

C_x	Biomass concentration ($kg.m^{-3}$)
D	Dilution rate (s^{-1})
G	Geometric factor, used to convert horizontal measured light radiation to a tilted surface (-)
I	Light intensity ($W.m^{-2}$)
I_{hor}	Measured light intensity on a horizontal surface ($W.m^{-2}$)
I_{PFD}	Photon flux density ($\mu mol.m^{-2}.s^{-1}$)
L	Straight tube length n loop (m)
K_a	Spectrally averaged absorption coefficient of algae ($m^2.kg^{-1}$)
N	Day number, 1st January is 1 (-)
P_{direct}	Length of light path (m)
P_m^C	Maximum carbon specific rate of photosynthesis (s^{-1})
R	Radius of the tube (m)
R_p	Reflection coefficient for *p*-polarized light (-)
R_s	Reflection coefficient for *s*-polarized light (-)
R_{tot}	Overall reflection coefficient for the air-reactor interface (-)
U_L	Superficial liquid velocity in the tube ($m.s^{-1}$)
$[O_2]_{in}$	Dissolved oxygen concentration at entrance of solar tube ($mol.L^{-1}$)
$[O_2]_{out}$	Dissolved oxygen concentration at the outlet of solar tube ($mol.L^{-1}$)
R_{O2}	Volumetric rate of oxygen generation (mol O_2 $m^{-3}.s^{-1}$)
h	Height of the reactor, equals two times the radius R (m)
h_{shadow}	Height of the shadow measured from the ground (m)
r_i	Radius describing points in circle (m)
t_{solar}	Solar time (h)
v	Liquid velocity ($m.s^{-1}$)
u	Sky view angle (°)

Greek letters

Θ	Chlorophyll *a* and carbon ratio in the cell (g Chl *a* g^{-1} C)
Θ_{max}	Maximal chlorophyll *a* and carbon ratio in the cell (g Chl *a* g^{-1} C)
α_v	Solar elevation, angle between the direction of the sun and the horizontal (the complement of the zenith angle) (°)
β	Slope of point on reactor, angle that the reactor surface makes with the surface of the earth (°)
γ	Azimuth angle, angle between the normal of the reactor orientation and the line due south, with negative angles towards the east and positive angles for the est (°)
δ	Declination of the sun, angular position (°) of the sun at solar noon with respect to the plane of the equator, for locations on the northern hemisphere the angle is positive and for the southern hemisphere the angle is negative
ε	Angle describing each point in the circle and on the contour of the circle in polar coordinates (°)
η_i	Refractive index of material before interface (-)
η_t	Refractive index of material after interface (-)
ξ	‘ true day’
θ	Angle of incidence, the angle between the sun rays and the normal of the reactor surface (°)
θ_i	Angle of incoming light (°)
θ_t	Angle of refraction (°)
θ_z	Zenith angle, the angle of incidence on a horizontal surface
K	Meridian to which the reactor location belongs (°)
σ	Functional cross section of the photosynthesis apparatus (g C (mol^{-1} photons) m^2g^{-1} Chl *a*)
τ	Distance between parallel tube (m)
λ	Longitude of the reactor location based on the prime meridian (East-positive, West-negative) (°)
μ	Growth rate (s^{-1})
μ_{max}	Maximal growth rate (s^{-1})
φ	Latitude of the reactor location for locations on the northern hemisphere the angle is positive and for the southern hemisphere the angle is negative (°)
ω	Hour angle, angular displacement of the sun from the local meridian caused by the rotation of the earth on its axis, the angle in negative in the morning and positive after noon (°)

Subscripts

Direct	Direct light
Diffuse	Diffuse light, solar light scattered by the atmosphere
Ground	Reflected light by the ground
Reflected	Solar radiation that is reflected by the ground, it is assumed to be diffuse
Tube	Reflected light by the tube